mathematics

MDPI

Article

Nonlinear Position Control Using Only Position Feedback under Position Errors and Yaw Constraints for Air Bearing Planar Motors

Wonhee Kim [1], Donghoon Shin [2] and Youngwoo Lee [3,*]

1 School of Energy Systems Engineering, Chung-Ang University, Seoul 06974, Korea; whkim79@cau.ac.kr
2 Global R&D Center, MANDO Corporation, Seongnam 463-400, Korea; donghoon.shin@halla.com
3 Department of Electrical Engineering, Chonnam National University, Gwangju 61186, Korea
* Correspondence: stork@jnu.ac.kr

Received: 10 July 2020; Accepted: 10 August 2020; Published: 13 August 2020

Abstract: In this paper, we propose a nonlinear position control using only position feedback to guarantee the tolerances for position tracking errors and yaw. In the proposed method, both mechanical and electrical dynamics are considered. The proposed method consists of the nonlinear position controller and nonlinear observer. The nonlinear position controller is designed by a backstepping procedure using the barrier Lyapunov function to satisfy the constraints of position error and yaw. The nonlinear observer is developed to estimate full state using only position feedback. The stability of the closed-loop system is proven using Lyapunov and input-to-state stabilities. Consequently, the proposed method satisfies the constraints of position error and yaw using only position feedback for the planar motor.

Keywords: planar motor; position control; observer

1. Introduction

A planar motor is a dual-axis linear motion motor that plays a significant role not only in semiconductor manufacturing systems and precision machine tools but also in automated assemblies.

A planar motor consists of four forcers that are symmetrically mounted on a puck, as shown in Figure 1 [1]. The position sensors are mounted on the puck to measure the positions for X and Y directions. Two position sensors are inserted in planar motor to calculate yaw angle using position difference between two position sensors in X direction. Each forcer is a one-axis force generation device. Forcers X_1 and X_2 generate force in the X direction whereas forcers Y_1 and Y_2 generate force in the Y direction. Yaw (θ) is generated by asymmetries in the forcers and leads to loss of synchronization between motor and platen teeth. It is undesirable and results in a severe force drop problem for electro-magnetic force. These forcers can be operated as stepper motors. The linear motion is achieved by the application of a proper sequence of phase currents. The planar motor operates on a steel waffle platen and is floated on the platen by an air bearing. This planar motor has three degrees of freedom that consists of two translational degrees of freedom and an unwanted rotational degree of freedom (yaw) due to the fact that not all forcers can be mounted at the center of mass. This forcer is capable of high position resolution (2 μm) and high speed moves (1 m/s) using open-loop microstepping. However, when these forcers are operated by open-loop microstepping, they may miss steps, or have long settle times Furthermore, the undesired rotation (yaw) produced by the asynchronous mounted forcers at the center of mass cannot be regulated by open-loop microstepping.

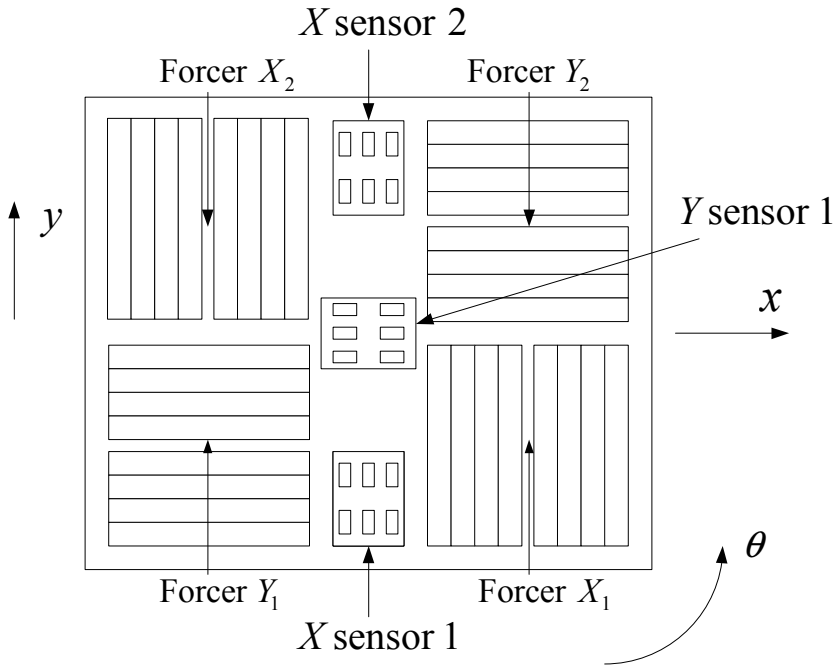

Figure 1. Bottom view of a planar motor.

Various feedback control methods have been proposed to control planar motors [2–6]. A robust adaptive control was designed to improve the position tracking performance [2]. In Reference [3], a proportional-integral-derivative (PID) controller with a velocity estimator was developed to reduce the settling time. An adaptive variable structure controller was proposed to guarantees global asymptotic tracking of a reference trajectory in [4]. A robust backstepping method was proposed to control planar motors without parameter information and current measurements [5]. The lead and proportional-integral (PI) compensators were proposed to satisfy phase margin for planar motors [6]. A learning adaptive robust control motion controller was proposed for a magnetically levitated planar motor to achieve good tracking performance [7]. In Reference [8], a predictive position control method using trajectory gradient soft constraint with attenuation coefficients in the weighting matrix to achieve high-precision, time-varying, and long-stroke positioning was proposed for planar motors.

These methods improved the position tracking performance; however, several drawbacks still exist. First, for planar motor control, satisfying the constraint of yaw regulation is important to avoid step-out. The previously reported methods have improved the position control performance; however, the constraining of the yaw cannot be guaranteed by these methods. Furthermore, the position tracking error constraints in both X and Y directions are also important. These constraints may be satisfied by the use of high gain in the controller. However, the use of high gain amplifies the ripple because of modeling errors, parameter uncertainties, and measurement noise [9]; thus, the system may become unstable. In addition, it may also result in peaking phenomenon; thus, the lateral control in the transient response becomes poor. Thus, the design of the control method is required to satisfy the constrains of the outputs [10–14]. Furthermore, in the previous methods, the currents are regarded as the inputs of the planar motor because electrical dynamics are faster than mechanical dynamics. That is, the electrical dynamics are neglected. However, when current control is used, the phase currents are reduced by back-back electromotive forces (EMFs) and have phase lags because of inductances [15]. Therefore, a feedback controller considering electrical dynamics is required for improving the control performance of planar motors [16]. A robust adaptive control with the consideration of electrical dynamics was proposed for planar motors [16]. However, this method required full state feedback. Generally, the position can be obtained by using a laser interferometer, and subsequently, the velocity is estimated. Normally, the currents are measured using sensing resistors. However, high-frequency

noises affect current measurements [17]; thus, an estimation of currents is necessary. To the best of our knowledge, there is no method to estimate full state using only position feedback for planar motors.

In this paper, we propose a nonlinear position control using only position feedback under the position errors and yaw constraints for air-bearing planar motors. In the proposed method, both mechanical and electrical dynamics are considered. The proposed method consists of the nonlinear position controller and nonlinear observer. The nonlinear position controller is designed using a backstepping procedure using barrier Lyapunov function (BLF) to satisfy the constraints of position errors and yaw. The nonlinear observer is developed to estimate full state using only position feedback. The stability of the closed-loop system is proven using Lyapunov stability and input-to-state stability (ISS). Consequently, the proposed method satisfies the constraints of position error and yaw using only position feedback for planar motors. The proposed method is validated via simulations. The main contributions of the proposed method can be summarized as follows:

- The whole dynamics including both the mechanical and the electrical dynamics is considered in the controller design.
- The tolerance for position tracking errors and yaw are guaranteed using only position feedback in the proposed method.
- The estimated state variables are used instead of the measured signals so that the measurement noise cannot affect the control performance.

2. Mathematical Model of Planar Motor

The planar motor consists of four forcers (X_1, X_2, Y_1, and Y_2) symmetrically mounted on a puck. The principles of each forcer are similar to those of a permanent magnet stepper motor. The electrical dynamics of the forcer X_1 is expressed [5] as follows:

$$\begin{aligned} \dot{i}_{x_{1a}} &= \frac{1}{L}[v_{x_{1a}} - Ri_{x_{1a}} - \kappa\dot{x}_1 \cos(\gamma x_1)] \\ \dot{i}_{x_{1b}} &= \frac{1}{L}[v_{x_{1b}} - Ri_{x_{1b}} - \kappa\dot{x}_1 \sin(\gamma x_1)], \end{aligned} \tag{1}$$

where x_1 is the position of the forcer X_1, $i_{x_{1a}}$ and $i_{x_{1b}}$ are the currents in the forcer X_1, $v_{x_{1a}}$ and $v_{x_{1b}}$ are the voltage inputs in the forcer X_1, κ is the force constant, R is the resistance of winding, L is the inductance, and $\gamma = \frac{2\pi}{p}$ where p is the toothpitch. The electrical dynamics of the other forcers X_2, Y_1, and Y_2 are the same as those of X_1. The forces, F_{x_1}, F_{x_2}, F_{y_1}, and F_{y_2}, are generated by the forcers X_1, X_2, Y_1 and Y_2, respectively, as follows:

$$\begin{aligned} F_{x_1} &= \kappa(i_{x_{1a}} \cos(\gamma x_1) + i_{x_{1b}} \sin(\gamma x_1)) \\ F_{x_2} &= \kappa(i_{x_{2a}} \cos(\gamma x_2) + i_{x_{2b}} \sin(\gamma x_2)) \\ F_{y_1} &= \kappa(i_{y_{1a}} \cos(\gamma y_1) + i_{y_{1b}} \sin(\gamma y_1)) \\ F_{y_2} &= \kappa(i_{y_{2a}} \cos(\gamma y_2) + i_{y_{2b}} \sin(\gamma y_2)). \end{aligned} \tag{2}$$

The total forces F_x and F_y in the X and Y directions, and the torque τ are calculated as follows:

$$\begin{aligned} F_x &= F_{x_1} + F_{x_2} \\ F_y &= F_{y_1} + F_{y_2} \\ \tau &= (F_{x_1} - F_{x_2})r + (F_{y_1} - F_{y_1})r, \end{aligned} \tag{3}$$

where r is the distance from the center of the motor to the forcer. Therefore, the dynamics of the planar motor are obtained as

$$
\begin{aligned}
\dot{x} &= x_v \\
\dot{x}_v &= \frac{1}{M}(F_x - \eta_x x_v) \\
\dot{y} &= y_v \\
\dot{y}_v &= \frac{1}{M}(F_y - \eta_y y_v) \\
\dot{\theta} &= \theta_v \\
\dot{\theta}_v &= \frac{1}{I}(\tau - \eta_\theta \theta_v) \\
\dot{i}_{x_{1a}} &= \frac{1}{L}[v_{x_{1a}} - Ri_{x_{1a}} - \kappa x_{1_v}\cos(\gamma x_1)] \\
\dot{i}_{x_{1b}} &= \frac{1}{L}[v_{x_{1b}} - Ri_{x_{1b}} - \kappa x_{1_v}\sin(\gamma x_1)] \\
\dot{i}_{x_{2a}} &= \frac{1}{L}[v_{x_{2a}} - Ri_{x_{2a}} - \kappa x_{2_v}\cos(\gamma x_2)] \\
\dot{i}_{x_{2b}} &= \frac{1}{L}[v_{x_{2b}} - Ri_{x_{2b}} - \kappa x_{2_v}\sin(\gamma x_2)] \\
\dot{i}_{y_{1a}} &= \frac{1}{L}[v_{y_{1a}} - Ri_{y_{1a}} - \kappa y_{1_v}\cos(\gamma y_1)] \\
\dot{i}_{y_{1b}} &= \frac{1}{L}[v_{y_{1b}} - Ri_{y_{1b}} - \kappa y_{1_v}\sin(\gamma y_1)] \\
\dot{i}_{y_{2a}} &= \frac{1}{L}[v_{y_{2a}} - Ri_{y_{2a}} - \kappa y_{2_v}\cos(\gamma y_2)] \\
\dot{i}_{y_{2b}} &= \frac{1}{L}[v_{y_{2b}} - Ri_{y_{2b}} - \kappa y_{2_v}\sin(\gamma y_2)],
\end{aligned}
\tag{4}
$$

where x is the X axis position of the center of the puck, y is the Y axis position of the center of the puck, and θ is the yaw rotation. $x_1 = x + r\sin(\theta)$, $x_2 = x - r\sin(\theta)$, $y_1 = y + r\sin(\theta)$, and $y_2 = y - r\sin(\theta)$ are the positions of force X_1, X_2, Y_1, and Y_2, respectively. x_{1_v}, x_{2_v}, y_{1_v}, and y_{2_v} are the linear velocity of the forcers, θ_v is the angular velocity of the yaw rotation. i_i's represent the currents in the forcers, v_i's represent the voltage inputs in the forcers, and, η_x, η_y, and η_θ are the coefficient of viscous friction.

3. Nonlinear Position Controller Design

3.1. Backstepping Control Using BLF for Mechanical Dynamics

In this subsection, the mechanical controllers are derived by a backstepping procedure using the BLF. In the context of mechanical dynamics, F_x, F_y, and τ can be regarded as virtual inputs, which are expressed as follows:

$$
\begin{aligned}
\dot{x} &= x_v \\
\dot{x}_v &= \frac{1}{M}(F_x - \eta_x x_v) \\
\dot{y} &= y_v \\
\dot{y}_v &= \frac{1}{M}(F_y - \eta_y y_v) \\
\dot{\theta} &= \theta_v \\
\dot{\theta}_v &= \frac{1}{I}(\tau - \eta_\theta \theta_v).
\end{aligned}
\tag{5}
$$

The mechanical errors are defined as

$$\begin{aligned} e_x &= x - x^d \\ e_{x_v} &= x_v - x_v^* \\ e_y &= y - y^d \\ e_{y_v} &= y_v - y_v^* \\ e_\theta &= \theta - \theta^d \\ e_{\theta_v} &= \theta_v - \theta_v^*, \end{aligned} \tag{6}$$

where x^d and y_d are the desired positions; and θ_d is the desired yaw, which is generally zero. Furthermore, x_v^*, y_v^*, and θ_v^* will be defined. The mechanical error dynamics are expressed as follows:

$$\begin{aligned} \dot{e}_x &= x_v - \dot{x}_d \\ \dot{e}_{x_v} &= \frac{1}{M}(F_x - \eta_x x_v) - \dot{x}_v^* \\ \dot{e}_y &= y_v - \dot{y}_d \\ \dot{e}_{y_v} &= \frac{1}{M}(F_y - \eta_y y_v) - \dot{y}_v^* \\ \dot{e}_\theta &= \theta_v - \dot{\theta}_d \\ \dot{e}_{\theta_v} &= \frac{1}{I}(\tau - \eta_\theta \theta_v) - \dot{\theta}_v^*. \end{aligned} \tag{7}$$

Theorem 1. *Consider the mechanical error dynamics (7) with $|e_x(0)| < b_x$, $|e_y(0)| < b_y$, and $|e_\theta(0)| < b_\theta$ where b_x, b_y, and b_θ are the positive constants and tolerances of the constraints for e_x, e_y, and e_θ, respectively. If the virtual inputs are expressed as follows:*

$$\begin{aligned} x_v^* &= -k_x e_x (b_x^2 - e_x^2) + \dot{x}_d \\ y_v^* &= -k_y e_y (b_y^2 - e_y^2) + \dot{y}_d \\ \theta_v^* &= -k_\theta e_\theta (b_\theta^2 - e_\theta^2) + \dot{\theta}_d, \end{aligned} \tag{8}$$

$$\begin{aligned} F_x &= -k_{x_v} e_{x_v} + \eta_x x_v + M\dot{x}_v^* - \frac{e_x}{b_x^2 - e_x^2} \\ F_y &= -k_{y_v} e_{y_v} + \eta_y y_v + M\dot{y}_v^* - \frac{e_x}{b_y^2 - e_y^2} \\ \tau &= -k_{\theta_v} e_{\theta_v} + \eta_\theta \theta_v + I\dot{\theta}_v^* - \frac{e_\theta}{b_\theta^2 - e_\theta^2}, \end{aligned} \tag{9}$$

where k_x, k_{x_v} , k_y, k_{y_v}, k_θ, and k_{θ_v} are the positive controller gains that are applied to the mechanical tracking error dynamics (7), then $|e_x(t)| < b_x$, $|e_y(t)| < b_y$, and $|e_\theta(t)| < b_\theta$, $\forall t > 0$ and $e_x(t)$, $e_y(t)$, and $e_\theta(t)$ asymptotically converge to zero.

Proof of Theorem 1. The BLF, V_{m_1}, is defined as

$$\begin{aligned} V_{m_1} =& \frac{1}{2}\log\left(\frac{b_x^2}{b_x^2 - e_x^2}\right) + \frac{1}{2}\log\left(\frac{b_y^2}{b_y^2 - e_y^2}\right) \\ &+ \frac{1}{2}\log\left(\frac{b_x^2}{b_x^2 - e_x^2}\right). \end{aligned} \tag{10}$$

The derivative of V_{m_1} with respect to time is given by

$$\begin{aligned}\dot{V}_{m_1} =& \frac{e_x\dot{e}_x}{b_x^2 - e_x^2} + \frac{e_y\dot{e}_y}{b_y^2 - e_y^2} + \frac{e_\theta\dot{e}_\theta}{b_\theta^2 - e_\theta^2} \\ =& \frac{e_x(x_v^* + e_{x_v} - \dot{x}_d)}{b_x^2 - e_x^2} + \frac{e_y(x_y^* + e_{x_y} - \dot{y}_d)}{b_y^2 - e_y^2} \\ &+ \frac{e_\theta(\theta_v^* + e_{\theta_v} - \dot{\theta}_d)}{b_\theta^2 - e_\theta^2}.\end{aligned} \tag{11}$$

With x_v^*, y_v^*, and θ_v^* (8), $\dot{V}_{m_1}$ becomes

$$\dot{V}_{m_1} = -k_x e_x^2 + \frac{e_x e_{x_v}}{b_x^2 - e_x^2} - k_y e_y^2 + \frac{e_y e_{y_v}}{b_y^2 - e_y^2} - k_\theta e_\theta^2 + \frac{e_\theta e_{\theta_v}}{b_\theta^2 - e_\theta^2}. \tag{12}$$

Let us define V_{m_2} as

$$V_{m_2} = V_{m_1} + \frac{1}{2}e_{x_v}^2 + \frac{1}{2}e_{x_y}^2 + \frac{1}{2}e_{\theta_v}^2. \tag{13}$$

We obtain $\dot{V}_{m_2}$ as

$$\begin{aligned}\dot{V}_{m_2} =& -k_x e_x^2 + \frac{e_x e_{x_v}}{b_x^2 - e_x^2} + e_{x_v}\dot{e}_{x_v} - k_y e_y^2 + \frac{e_y e_{y_v}}{b_y^2 - e_y^2} + e_{y_v}\dot{e}_{y_v} \\ &- k_\theta e_\theta^2 + \frac{e_\theta e_{\theta_v}}{b_\theta^2 - e_\theta^2} + e_{\theta_v}\dot{e}_{\theta_v} \\ =& -k_x e_x^2 + \frac{e_x e_{x_v}}{b_x^2 - e_x^2} + e_{x_v}\left(\frac{1}{M}(F_x - \eta_x x_v) - \dot{x}_v^*\right) \\ &- k_y e_y^2 + \frac{e_y e_{y_v}}{b_y^2 - e_y^2} + e_{y_v}\left(\frac{1}{M}(F_y - \eta_y y_v) - \dot{y}_v^*\right) \\ &- k_\theta e_\theta^2 + \frac{e_\theta e_{\theta_v}}{b_\theta^2 - e_\theta^2} + e_{\theta_v}\left(\frac{1}{I}(\tau - \eta_\theta \theta_v) - \dot{\theta}_v^*\right).\end{aligned} \tag{14}$$

With virtual inputs (9), $\dot{V}_{m_2}$ becomes

$$\dot{V}_{m_2} = -k_x e_x^2 - k_y e_y^2 - k_\theta e_\theta^2 - k_{x_v} e_{x_v}^2 - k_{y_v} e_{y_v}^2 - k_{\theta_v} e_{\theta_v}^2. \tag{15}$$

Thus, $|e_x(t)| < b_x$, $|e_y(t)| < b_y$, and $|e_\theta(t)| < b_\theta$, $\forall t > 0$ and $e_x(t)$, $e_y(t)$, and $e_\theta(t)$ converge to zero. □

Note that F_x, F_y, and τ are not actual inputs in the mechanical dynamics (5). Thus, the virtual inputs (9) are the desired X-axis and Y-axis forces and torque, which are expressed as follows:

$$\begin{aligned}F_x^d &= -k_{x_v} e_{x_v} + \eta_x x_v + M\dot{x}_v^* - \frac{e_x}{b_x^2 - e_x^2} \\ F_y^d &= -k_{y_v} e_{y_v} + \eta_y y_v + M\dot{y}_v^* - \frac{e_x}{b_y^2 - e_y^2} \\ \tau^d &= -k_{\theta_v} e_{\theta_v} + \eta_\theta \theta_v + I\dot{\theta}_v^* - \frac{e_\theta}{b_\theta^2 - e_\theta^2}.\end{aligned} \tag{16}$$

Note that the desired X-axis and Y-axis forces and torque can guarantee the constraints of e_x, e_y, and e_θ.

3.2. Commutation Scheme

In the planar motor, the actual inputs are voltages and not forces and torque. To obtain the desired forces and torque, the desired currents are defined as follows:

$$\begin{aligned}
i^d_{x_{1a}} &= \left(\frac{F^d_x}{2\kappa} + \frac{\tau^d}{4\kappa r}\right)\cos(\gamma x_1)\\
i^d_{x_{1b}} &= \left(\frac{F^d_x}{2\kappa} + \frac{\tau^d}{4\kappa r}\right)\sin(\gamma x_1)\\
i^d_{x_{2a}} &= \left(\frac{F^d_x}{2\kappa} - \frac{\tau^d}{4\kappa r}\right)\cos(\gamma x_2)\\
i^d_{x_{2b}} &= \left(\frac{F^d_x}{2\kappa} - \frac{\tau^d}{4\kappa r}\right)\sin(\gamma x_2)\\
i^d_{y_{1a}} &= \left(\frac{F^d_y}{2\kappa} + \frac{\tau^d}{4\kappa r}\right)\cos(\gamma y_1)\\
i^d_{y_{1b}} &= \left(\frac{F^d_y}{2\kappa} + \frac{\tau^d}{4\kappa r}\right)\sin(\gamma y_1)\\
i^d_{y_{2a}} &= \left(\frac{F^d_y}{2\kappa} - \frac{\tau^d}{4\kappa r}\right)\cos(\gamma y_2)\\
i^d_{y_{2b}} &= \left(\frac{F^d_y}{2\kappa} - \frac{\tau^d}{4\kappa r}\right)\sin(\gamma y_2)
\end{aligned} \tag{17}$$

where i^d_i, $i \in [x_{1a}, x_{1b}, x_{2a}, x_{2b}, y_{1a}, y_{1b}, y_{2a}, y_{2b}]$, are the desired phase currents.

3.3. Nonlinear Current Controllers for Electrical Dynamics

The phase currents of the planar motor decreased because of back-EMFs and have phase lags by inductances during operation. Now, we design the nonlinear controller to guarantee the desired currents (17) for the electrical dynamics controller. First, we design the controller for the forcer X_1. Let us define the current errors for the forcer X_1 as follows:

$$\begin{aligned}
e_{x_{1a}} &= i_{x_{1a}} - i^d_{x_{1a}}\\
e_{x_{1b}} &= i_{x_{1b}} - i^d_{x_{1b}}.
\end{aligned} \tag{18}$$

The current error dynamics for the forcer X_1 are

$$\begin{aligned}
\dot{e}_{x_{1a}} &= \frac{1}{L}[v_{x_{1a}} - Ri_{x_{1a}} - \kappa x_{1_v}\cos(\gamma x_1)] - \dot{i}^d_{x_{1a}}\\
\dot{e}_{x_{1b}} &= \frac{1}{L}[v_{x_{1b}} - Ri_{x_{1b}} - \kappa x_{1_v}\sin(\gamma x_1)] - \dot{i}^d_{x_{1b}}.
\end{aligned} \tag{19}$$

Theorem 2. *Consider the current error dynamics for the forcer* X_1 (19). *If the voltage inputs for the forcer* X_1 *are given by*

$$\begin{aligned}
v_{x_{1a}} &= (Ri_{x_{1a}} + \kappa x_{1_v}\cos(\gamma x_1)) + L(\dot{i}^d_{x_{1a}} - k_e e_{x_{1a}})\\
v_{x_{1b}} &= (Ri_{x_{1b}} + \kappa x_{1_v}\sin(\gamma x_1)) + L(\dot{i}^d_{x_{1b}} - k_e e_{x_{1b}}),
\end{aligned} \tag{20}$$

where k_e is a positive controller gain applied to the current error dynamics for the forcer X_1 (19), then $e_{x_{1a}}$ and $e_{x_{1b}}$ exponentially converge to zero.

Proof of Theorem 2. The Lyapunov candidate function, V_e is defined as

$$V_e = \frac{1}{2}e_{x_{1a}}^2 + \frac{1}{2}e_{x_{1b}}^2. \tag{21}$$

Differentiating V_e (21) yields

$$\begin{aligned}\dot{V} =& e_{x_{1a}}(\dot{i}_{x_{1a}} - \dot{i}_{x_{1a}}^d) + e_{x_{1b}}(\dot{i}_{x_{1b}} - \dot{i}_{x_{1b}}^d)\\ =& e_{x_{1a}}(\frac{1}{L}[v_{x_{1a}} - Ri_{x_{1a}} - \kappa x_{1_v}\cos(\gamma x_1)] - \dot{i}_{x_{1a}}^d)\\ &+ e_{x_{1b}}(\frac{1}{L}[v_{x_{1b}} - Ri_{x_{1b}} - \kappa x_{1_v}\sin(\gamma x_1)] - \dot{i}_{x_{1b}}^d).\end{aligned} \tag{22}$$

With the nonlinear controller (20), $\dot{V}_e$ becomes

$$\dot{V}_e = -k_e e_{x_{1a}}^2 - k_e e_{x_{1b}}^2. \tag{23}$$

□

The electrical dynamics of the forcers X_1, X_2, X_3 and X_4 are all the same, thus the controllers for other forces are analogous to (20). From the controller for the forcers X_1, the controllers for all forcers X_1, X_2, X_3 and X_4 can be designed as

$$\begin{aligned}v_{x_{1a}} =& (Ri_{x_{1a}} + \kappa x_{1_v}\cos(\gamma x_1)) + L(\dot{v}_{x_{1a}}^d - k_e e_{x_{1a}})\\ v_{x_{1b}} =& (Ri_{x_{1b}} + \kappa x_{1_v}\sin(\gamma x_1)) + L(\dot{v}_{x_{1b}}^d - k_e e_{x_{1b}})\\ v_{x_{2a}} =& (Ri_{x_{2a}} + \kappa x_{2_v}\cos(\gamma x_1)) + L(\dot{v}_{x_{2a}}^d - k_e e_{x_{2a}})\\ v_{x_{2b}} =& (Ri_{x_{2b}} + \kappa x_{2_v}\sin(\gamma x_2)) + L(\dot{v}_{x_{2b}}^d - k_e e_{x_{2b}})\\ v_{y_{1a}} =& (Ri_{y_{1a}} + \kappa y_{1_v}\cos(\gamma y_1)) + L(\dot{v}_{y_{1a}}^d - k_e e_{y_{1a}})\\ v_{y_{1b}} =& (Ri_{y_{1b}} + \kappa y_{1_v}\sin(\gamma y_1)) + L(\dot{v}_{y_{1b}}^d - k_e e_{y_{1b}})\\ v_{y_{2a}} =& (Ri_{y_{2a}} + \kappa y_{2_v}\cos(\gamma y_1)) + L(\dot{v}_{y_{2a}}^d - k_e e_{y_{2a}})\\ v_{y_{2b}} =& (Ri_{y_{2b}} + \kappa y_{2_v}\sin(\gamma y_2)) + L(\dot{v}_{y_{2b}}^d - k_e e_{y_{2b}}).\end{aligned} \tag{24}$$

4. Observer Design

In the previous section, for the proposed controller design, we assumed that the full states are measurable. In this paper, we assume that the positions for X and Y directions are measurable, that is, x, y, and θ are available. $x_{1_v} = x_v + r\dot{\theta}\cos(\theta)$, $x_{2_v} = x_v - r\dot{\theta}\cos(\theta)$, $y_{1_v} = y_v + r\dot{\theta}\cos(\theta)$, and $y_{2_v} = y_v - r\dot{\theta}\cos(\theta)$; thus, the dynamics of the planar motor (4) can be rewritten as

$$\begin{aligned}\dot{x} =& \quad x_v\\ \dot{x}_v =& \quad \tfrac{1}{M}(F_x - \eta_x x_v)\\ \dot{y} =& \quad y_v\\ \dot{y}_v =& \quad \tfrac{1}{M}(F_y - \eta_y y_v)\\ \dot{\theta} =& \quad \theta_v\\ \dot{\theta}_v =& \quad \tfrac{1}{I}(\tau - \eta_\theta \theta_v)\\ \dot{i}_{x1a} =& \quad \tfrac{1}{L}[v_{x1a} - Ri_{x1a} - \kappa x_v\cos(\gamma x_1) - \kappa r\theta_v\cos(\theta)\cos(\gamma x_1)]\\ \dot{i}_{x1b} =& \quad \tfrac{1}{L}[v_{x1b} - Ri_{x1b} - \kappa x_v\sin(\gamma x_1) - \kappa r\theta_v\cos(\theta)\sin(\gamma x_1)]\\ \dot{i}_{x2a} =& \quad \tfrac{1}{L}[v_{x2a} - Ri_{x2a} - \kappa x_v\cos(\gamma x_2) + \kappa r\theta_v\cos(\theta)\cos(\gamma x_2)]\\ \dot{i}_{x2b} =& \quad \tfrac{1}{L}[v_{x2b} - Ri_{x2b} - \kappa x_v\sin(\gamma x_2) + \kappa r\theta_v\cos(\theta)\sin(\gamma x_2)]\\ \dot{i}_{y1a} =& \quad \tfrac{1}{L}[v_{y1a} - Ri_{y1a} - \kappa y_v\cos(\gamma y_1) - \kappa r\theta_v\cos(\theta)\cos(\gamma y_1)]\\ \dot{i}_{y1b} =& \quad \tfrac{1}{L}[v_{y1b} - Ri_{y1b} - \kappa y_v\sin(\gamma y_1) - \kappa r\theta_v\cos(\theta)\sin(\gamma y_1)]\\ \dot{i}_{y2a} =& \quad \tfrac{1}{L}[v_{y2a} - Ri_{y2a} - \kappa y_v\cos(\gamma y_2) + \kappa r\theta_v\cos(\theta)\cos(\gamma y_2)]\\ \dot{i}_{y2b} =& \quad \tfrac{1}{L}[v_{y2b} - Ri_{y2b} - \kappa y_v\sin(\gamma y_2) + \kappa r\theta_v\cos(\theta)\sin(\gamma y_2)].\end{aligned} \tag{25}$$

We proposed a nonlinear observer to estimate the full states as follows:

$$
\begin{aligned}
\dot{\hat{x}} =& \hat{x}_v + l_x(x - \hat{x}) \\
\dot{\hat{x}}_v =& \frac{1}{M}[\hat{F}_x - \eta_x \hat{x}_v] + l_{xv}(x - \hat{x}) \\
\dot{\hat{y}} =& \hat{y}_v + l_y(y - \hat{y}) \\
\dot{\hat{y}}_v =& \frac{1}{M}[\hat{F}_y - \eta_y \hat{y}_v] + l_{yv}(y - \hat{y}) \\
\dot{\hat{\theta}} =& \hat{\theta}_v + l_\theta(\theta - \hat{\theta}) \\
\dot{\hat{\theta}}_v =& \frac{1}{I}[\hat{\tau} - \eta_\theta \hat{\theta}_v] + l_{\theta v}(\theta - \hat{\theta}) \\
\dot{\hat{i}}_{x1a} =& \frac{1}{L}[v_{x1a} - R\hat{i}_{x1a} - \kappa \hat{x}_v \cos(\gamma x_1) - \kappa r \hat{\theta}_v \cos(\theta)\cos(\gamma x_1)] \\
& + l_{x1a}(x - \hat{x}) \\
\dot{\hat{i}}_{x1b} =& \frac{1}{L}[v_{x1b} - R\hat{i}_{x1b} - \kappa \hat{x}_v \sin(\gamma x_1) - \kappa r \hat{\theta}_v \cos(\theta)\sin(\gamma x_1)] \\
& + l_{x1b}(x - \hat{x}) \\
\dot{\hat{i}}_{x2a} =& \frac{1}{L}[v_{x2a} - R\hat{i}_{x2a} - \kappa \hat{x}_v \cos(\gamma x_2) + \kappa r \hat{\theta}_v \cos(\theta)\cos(\gamma x_2)] \\
& + l_{x2a}(x - \hat{x}) \\
\dot{\hat{i}}_{x2b} =& \frac{1}{L}[v_{x2b} - R\hat{i}_{x2b} - \kappa \hat{x}_v \sin(\gamma x_2) + \kappa r \hat{\theta}_v \cos(\theta)\sin(\gamma x_2)] \\
& + l_{x2b}(x - \hat{x}) \\
\dot{\hat{i}}_{y1a} =& \frac{1}{L}[v_{y1a} - R\hat{i}_{y1a} - \kappa \hat{y}_v \cos(\gamma y_1) - \kappa r \hat{\theta}_v \cos(\theta)\cos(\gamma y_1)] \\
& + l_{y1a}(y - \hat{y}) \\
\dot{\hat{i}}_{y1b} =& \frac{1}{L}[v_{y1b} - R\hat{i}_{y1b} - \kappa \hat{y}_v \sin(\gamma y_1) - \kappa r \hat{\theta}_v \cos(\theta)\sin(\gamma y_1)] \\
& + l_{y1b}(y - \hat{y}) \\
\dot{\hat{i}}_{y2a} =& \frac{1}{L}[v_{y2a} - R\hat{i}_{y2a} - \kappa \hat{y}_v \cos(\gamma y_2) + \kappa r \hat{\theta}_v \cos(\theta)\cos(\gamma y_2)] \\
& + l_{y2a}(y - \hat{y}) \\
\dot{\hat{i}}_{y2b} =& \frac{1}{L}[v_{y2b} - R\hat{i}_{y2b} - \kappa \hat{y}_v \sin(\gamma y_2) + \kappa r \hat{\theta}_v \cos(\theta)\sin(\gamma y_2)] \\
& + l_{y2b}(y - \hat{y}),
\end{aligned}
\tag{26}
$$

where $\hat{\bullet}$ denotes the estimation of $\bullet$, $\hat{F}_x = \kappa(\hat{i}_{x1a}\cos(\gamma x_1) + \hat{i}_{x1b}\sin(\gamma x_1)) + \kappa(\hat{i}_{x2a}\cos(\gamma x_2) + \hat{i}_{x2b}\sin(\gamma x_2))$, $\hat{F}_y = \kappa(\hat{i}_{y1a}\cos(\gamma y_1) + \hat{i}_{y1b}\sin(\gamma y_1)) + \kappa(\hat{i}_{y2a}\cos(\gamma y_2) + \hat{i}_{y2b}\sin(\gamma y_2))$, $\hat{\tau} = [\kappa r(\hat{i}_{x1a}\cos(\gamma x_1) + \hat{i}_{x1b}\sin(\gamma x_1)) - \kappa r(\hat{i}_{x2a}\cos(\gamma x_2) + \hat{i}_{x1b}\sin(\gamma x_2))] + [\kappa r(\hat{i}_{y1a}\cos(\gamma y_1) + \hat{i}_{y1b}\sin(\gamma y_1)) - \kappa r(\hat{i}_{y2a}\cos(\gamma y_2) + \hat{i}_{y2b}\sin(\gamma y_2))]$. The estimation errors are defined as

$$\begin{aligned}
\tilde{x} =& x - \hat{x} \\
\tilde{y} =& y - \hat{y} \\
\tilde{\theta} =& \theta - \hat{\theta} \\
\tilde{i}_{x1a} =& i_{x1a} - \hat{i}_{x1a} \\
\tilde{i}_{x1b} =& i_{x1b} - \hat{i}_{x1b} \\
\tilde{i}_{x2a} =& i_{x2a} - \hat{i}_{x2a} \\
\tilde{i}_{x2b} =& i_{x2b} - \hat{i}_{x2a} \\
\tilde{i}_{y1a} =& i_{y1a} - \hat{i}_{y1a} \\
\tilde{i}_{y1b} =& i_{y1b} - \hat{i}_{y1b} \\
\tilde{i}_{y2a} =& i_{y2a} - \hat{i}_{y2a} \\
\tilde{i}_{y2b} =& i_{y2b} - \hat{i}_{y2a}.
\end{aligned} \tag{27}$$

The estimation error dynamics are obtained by

$$\begin{aligned}
\dot{\tilde{x}} =& \tilde{x}_v - l_x \tilde{x} \\
\dot{\tilde{x}}_v =& \frac{1}{M}[\tilde{F}_x - \eta_x \tilde{x}_v] - l_{xv} \tilde{x} \\
\dot{\tilde{y}} =& \tilde{y}_v - l_y \tilde{y} \\
\dot{\tilde{y}}_v =& \frac{1}{M}[\tilde{F}_y - \eta_y \tilde{y}_v] - l_{yv} \tilde{y} \\
\dot{\tilde{\theta}} =& \tilde{\theta}_v - l_\theta \tilde{\theta} \\
\dot{\tilde{\theta}}_v =& \frac{1}{I}[\tilde{\tau} - \eta_\theta \tilde{\theta}] - l_{\theta v} \tilde{\theta} \\
\dot{\tilde{i}}_{x1a} =& \frac{1}{L}[-R\tilde{i}_{x1a} - \kappa \tilde{x}_v \cos(\gamma x_1) - \kappa r \tilde{\theta}_v \cos(\theta)\cos(\gamma x_1)] - l_{x1a}\tilde{x} \\
\dot{\tilde{i}}_{x1b} =& \frac{1}{L}[-R\tilde{i}_{x1b} - \kappa \tilde{x}_v \sin(\gamma x_1) - \kappa r \tilde{\theta}_v \cos(\theta)\sin(\gamma x_1)] - l_{x1b}\tilde{x} \\
\dot{\tilde{i}}_{x2a} =& \frac{1}{L}[-R\tilde{i}_{x2a} - \kappa \tilde{x}_v \cos(\gamma x_2) + \kappa r \tilde{\theta}_v \cos(\theta)\cos(\gamma x_2)] - l_{x2a}\tilde{x} \\
\dot{\tilde{i}}_{x2b} =& \frac{1}{L}[-R\tilde{i}_{x2b} - \kappa \tilde{x}_v \sin(\gamma x_2) + \kappa r \tilde{\theta}_v \cos(\theta)\sin(\gamma x_2)] - l_{x2b}\tilde{x} \\
\dot{\tilde{i}}_{y1a} =& \frac{1}{L}[-R\tilde{i}_{y1a} - \kappa \tilde{y}_v \cos(\gamma y_1) - \kappa r \tilde{\theta}_v \cos(\theta)\cos(\gamma y_1)] - l_{y1a}\tilde{y} \\
\dot{\tilde{i}}_{y1b} =& \frac{1}{L}[-R\tilde{i}_{y1b} - \kappa \tilde{y}_v \sin(\gamma y_1) - \kappa r \tilde{\theta}_v \cos(\theta)\sin(\gamma y_1)] - l_{y1b}\tilde{y} \\
\dot{\tilde{i}}_{y2a} =& \frac{1}{L}[-R\tilde{i}_{y2a} - \kappa \tilde{y}_v \cos(\gamma y_2) + \kappa r \tilde{\theta}_v \cos(\theta)\cos(\gamma y_2)] - l_{y2a}\tilde{y} \\
\dot{\tilde{i}}_{y2b} =& \frac{1}{L}[-R\tilde{i}_{y2b} - \kappa \tilde{y}_v \sin(\gamma y_2) + \kappa r \tilde{\theta}_v \cos(\theta)\sin(\gamma y_2)] - l_{y2b}\tilde{y},
\end{aligned} \tag{28}$$

where $\tilde{F}_x = \kappa(\tilde{i}_{x1a}\cos(\gamma x_1) + \tilde{i}_{x1b}\sin(\gamma x_1)) + \kappa(\tilde{i}_{x2a}\cos(\gamma x_2) + \tilde{i}_{x2b}\sin(\gamma x_2))$, $\tilde{F}_y = \kappa(\tilde{i}_{y1a}\cos(\gamma y_1) + \tilde{i}_{y1b}\sin(\gamma y_1)) + \kappa(\tilde{i}_{y2a}\cos(\gamma y_2) + \tilde{i}_{y2b}\sin(\gamma y_2))$, $\tilde{\tau} = [\kappa r(\tilde{i}_{x1a}\cos(\gamma x_1) + \tilde{i}_{x1b}\sin(\gamma x_1)) - \kappa r(\tilde{i}_{x2a}\cos(\gamma x_2) + \tilde{i}_{x1b}\sin(\gamma x_2))] + [\kappa r(\tilde{i}_{y1a}\cos(\gamma y_1) + \tilde{i}_{y1b}\sin(\gamma y_1)) - \kappa r(\tilde{i}_{y2a}\cos(\gamma y_2) + \tilde{i}_{y2b}\sin(\gamma y_2))]$.

Assumption 1. *During the operation of the planar motor,* $\cos(\theta) \geq 0, \forall t > 0$. $\Diamond$ *The planar motor steps out when the yaw is relatively large. Thus, this assumption is reasonable.*

Theorem 3. *Suppose the estimation error dynamics* (28) *with Assumption 1. If* l_x, l_y, *and* l_θ *are positive,* l_{xv} *and* l_{yv} *are* $\frac{L}{M}$, *and* $l_{\theta v}$ *is* $\frac{L}{I}$, *then the estimation errors exponentially converge to zero.*

Proof of Theorem 3. The Lyapunov candidate function, V_o is defined as

$$\begin{aligned} V_o =& \frac{1}{2}(\tilde{x}^2 + \frac{M}{L}\tilde{x}_v^2 + \tilde{y}^2 + \frac{M}{L}\tilde{y}_v^2 + \tilde{\theta}^2 + \frac{I\cos(\theta)}{L}\tilde{\theta}_v^2 \\ &+ \tilde{i}_{x1a}^2 + \tilde{i}_{x1b}^2 + \tilde{i}_{x2a}^2 + \tilde{i}_{x2b}^2 + \tilde{i}_{y1a}^2 + \tilde{i}_{y1b}^2 + \tilde{i}_{y2a}^2 + \tilde{i}_{y2b}^2). \end{aligned} \tag{29}$$

with Assumption 1, (29) can be the Lyapunov candidate function. The derivative of V_o is as follows:

$$\begin{aligned} \dot{V}_0 =& -l_x\tilde{x}^2 - \frac{\eta_x}{L}\tilde{x}_v^2 - l_y\tilde{y}^2 - \frac{\eta_y}{L}\tilde{y}_v^2 - l_\theta\tilde{\theta}^2 + \frac{\eta_\theta}{L}\tilde{\theta}_v^2 \\ &- \frac{R}{L}\tilde{i}_{x1a}^2 - \frac{R}{L}\tilde{i}_{x1b}^2 - \frac{R}{L}\tilde{i}_{x2a}^2 - \frac{R}{L}\tilde{i}_{x2b}^2 \\ &- \frac{R}{L}\tilde{i}_{y1a}^2 - \frac{R}{L}\tilde{i}_{y1b}^2 - \frac{R}{L}\tilde{i}_{y2a}^2 - \frac{R}{L}\tilde{i}_{y2b}^2. \end{aligned} \tag{30}$$

If l_x, l_y, and l_θ are positive, l_{xv} and l_{yv} are $\frac{L}{M}$, and $l_{\theta v}$ is $\frac{L}{I}$, then $\dot{V}_o$ is negative definite. Thus, the estimation errors exponentially converge to zero. □

5. Analysis of Closed-Loop System

The backstepping controller (16), nonlinear controller (24), and nonlinear observer (26) were designed separately. Thus, the stability of the closed-loop system should be studied. The closed-loop system is expressed as follows:

$$\begin{aligned} \dot{e}_m =& A_m e_m + B_{m_1}(X)e_e + B_{m_2}\tilde{X} \\ \dot{e}_e =& A_e e_e + B_e(X)\tilde{X} \\ \dot{\tilde{X}} =& A_{ob}(X)\tilde{X}, \end{aligned} \tag{31}$$

where $e_m = [e_x \ e_{x_v} \ e_y \ e_{y_v} \ e_\theta \ e_{\theta_v}]^T$, $e_e = [e_{x_{1a}} \ e_{x_{1b}} \ e_{x_{2a}} \ e_{x_{2b}} \ e_{y_{1a}} \ e_{y_{1b}} \ e_{y_{2a}} \ e_{y_{2b}}]^T$, $X = [x \ x_v \ y \ y_v \ \theta \ \theta_v \ i_{x_{1a}} \ i_{x_{1b}} \ i_{x_{2a}} \ i_{x_{2b}}]^T$, $\tilde{X} = [\tilde{x} \ \tilde{x}_v \ \tilde{y} \ \tilde{y}_v \ \tilde{\theta} \ \tilde{\theta}_v \ \tilde{i}_{x_{1a}} \ \tilde{i}_{x_{1b}} \ \tilde{i}_{x_{2a}} \ \tilde{i}_{x_{2b}} \ \tilde{i}_{y_{1a}} \ \tilde{i}_{y_{1b}} \ \tilde{i}_{y_{2a}} \ \tilde{i}_{y_{2b}}]^T$, $c_{i_i} = \cos(\gamma i_j)$, $s_{i_i} = \sin(\gamma i_j)$ for $i \in [x, y]$ and $i \in [1, 2]$, $c_\theta = \cos(\theta)$, $b_{m_2} = -\frac{R}{L} + k_e$

$$A_m = \begin{bmatrix} -k_x & 0 & 0 & 0 & 0 & 0 \\ 0 & -k_{x_v} & 0 & 0 & 0 & 0 \\ 0 & 0 & -k_y & 0 & 0 & 0 \\ 0 & 0 & 0 & -k_{y_v} & 0 & 0 \\ 0 & 0 & 0 & 0 & -k_\theta & 0 \\ 0 & 0 & 0 & 0 & 0 & -k_{\theta_v} \end{bmatrix}$$

$$A_e = \begin{bmatrix} -k_e & 0 & 0 & 0 & 0 & 0 & 0 & 0 \\ 0 & -k_e & 0 & 0 & 0 & 0 & 0 & 0 \\ 0 & 0 & -k_e & 0 & 0 & 0 & 0 & 0 \\ 0 & 0 & 0 & -k_e & 0 & 0 & 0 & 0 \\ 0 & 0 & 0 & 0 & -k_e & 0 & 0 & 0 \\ 0 & 0 & 0 & 0 & 0 & -k_e & 0 & 0 \\ 0 & 0 & 0 & 0 & 0 & 0 & -k_e & 0 \\ 0 & 0 & 0 & 0 & 0 & 0 & 0 & -k_e \end{bmatrix}$$

$$B_{m_1}(X) = \begin{bmatrix} 0 & 0 & 0 & 0 & 0 & 0 & 0 & 0 \\ \frac{\kappa}{M}c_{x_1} & \frac{\kappa}{M}s_{x_1} & \frac{\kappa}{M}c_{x_2} & \frac{\kappa}{M}s_{x_2} & 0 & 0 & 0 & 0 \\ 0 & 0 & 0 & 0 & 0 & 0 & 0 & 0 \\ 0 & 0 & 0 & 0 & \frac{\kappa}{M}c_{y_1} & \frac{\kappa}{M}s_{y_1} & \frac{\kappa}{M}c_{y_2} & \frac{\kappa}{M}s_{y_2} \\ 0 & 0 & 0 & 0 & 0 & 0 & 0 & 0 \\ \frac{r\kappa}{M}c_{x_1} & \frac{r\kappa}{M}s_{x_1} & -\frac{r\kappa}{M}c_{x_2} & -\frac{r\kappa}{M}s_{x_2} & \frac{r\kappa}{M}c_{y_1} & \frac{r\kappa}{M}s_{y_1} & -\frac{r\kappa}{M}c_{y_2} & -\frac{r\kappa}{M}s_{y_2} \end{bmatrix}$$

$$B_{m_2} = \begin{bmatrix} 0 & 0 & 0 & 0 & 0 & 0 & 0 & 0 & 0 & 0 & 0 & 0 & 0 & 0 \\ 0 & \frac{\eta_x}{M} & 0 & 0 & 0 & 0 & 0 & 0 & 0 & 0 & 0 & 0 & 0 & 0 \\ 0 & 0 & 0 & 0 & 0 & 0 & 0 & 0 & 0 & 0 & 0 & 0 & 0 & 0 \\ 0 & 0 & 0 & \frac{\eta_y}{M} & 0 & 0 & 0 & 0 & 0 & 0 & 0 & 0 & 0 & 0 \\ 0 & 0 & 0 & 0 & 0 & 0 & 0 & 0 & 0 & 0 & 0 & 0 & 0 & 0 \\ 0 & 0 & 0 & 0 & 0 & \frac{\eta_\theta}{M} & 0 & 0 & 0 & 0 & 0 & 0 & 0 & 0 \end{bmatrix}$$

$$B_e(X) = \begin{bmatrix} 0 & -\frac{\kappa}{L}c_{x_1} & 0 & 0 & 0 & -\frac{r\kappa}{L}c_\theta c_{x_1} & b_{m_2} & 0 & 0 & 0 & 0 & 0 & 0 & 0 \\ 0 & -\frac{\kappa}{L}s_{x_1} & 0 & 0 & 0 & -\frac{r\kappa}{L}c_\theta s_{x_1} & 0 & b_{m_2} & 0 & 0 & 0 & 0 & 0 & 0 \\ 0 & -\frac{\kappa}{L}c_{x_2} & 0 & 0 & 0 & -\frac{r\kappa}{L}c_\theta c_{x_2} & 0 & 0 & b_{m_2} & 0 & 0 & 0 & 0 & 0 \\ 0 & -\frac{\kappa}{L}s_{x_2} & 0 & 0 & 0 & -\frac{r\kappa}{L}c_\theta s_{x_2} & 0 & 0 & 0 & b_{m_2} & 0 & 0 & 0 & 0 \\ 0 & 0 & 0 & -\frac{\kappa}{L}c_{y_1} & 0 & -\frac{r\kappa}{L}c_\theta c_{y_1} & 0 & 0 & 0 & 0 & b_{m_2} & 0 & 0 & 0 \\ 0 & 0 & 0 & -\frac{\kappa}{L}s_{y_1} & 0 & -\frac{r\kappa}{L}c_\theta s_{y_1} & 0 & 0 & 0 & 0 & 0 & b_{m_2} & 0 & 0 \\ 0 & 0 & 0 & -\frac{\kappa}{L}c_{y_2} & 0 & -\frac{r\kappa}{L}c_\theta c_{y_2} & 0 & 0 & 0 & 0 & 0 & 0 & b_{m_2} & 0 \\ 0 & 0 & 0 & -\frac{\kappa}{L}s_{y_2} & 0 & -\frac{r\kappa}{L}c_\theta s_{y_2} & 0 & 0 & 0 & 0 & 0 & 0 & 0 & b_{m_2} \end{bmatrix}$$

$$A_{ob} = \begin{bmatrix} -l_x & 1 & 0 & 0 & 0 & 0 & 0 & 0 & 0 & 0 & 0 & 0 & 0 & 0 \\ -l_{xv} & -\frac{\eta_x}{M} & 0 & 0 & 0 & 0 & \frac{\kappa}{M}c_{x_1} & \frac{\kappa}{M}s_{x_1} & \frac{\kappa}{M}c_{x_2} & \frac{\kappa}{M}s_{x_2} & 0 & 0 & 0 & 0 \\ 0 & 0 & -l_y & 1 & 0 & 0 & 0 & 0 & 0 & 0 & 0 & 0 & 0 & 0 \\ 0 & 0 & -l_{yv} & -\frac{\eta_y}{M} & 0 & 0 & 0 & 0 & 0 & \frac{\kappa}{M}c_{y_1} & \frac{\kappa}{M}s_{y_1} & \frac{\kappa}{M}c_{y_2} & \frac{\kappa}{M}s_{y_2} & \\ 0 & 0 & 0 & 0 & -l_\theta & 0 & 0 & 0 & 0 & 0 & 0 & 0 & 0 & 0 \\ 0 & 0 & 0 & 0 & -l_{\theta v} & -\frac{\eta_\theta}{I} & \frac{r\kappa}{I}c_{x_1} & \frac{r\kappa}{I}s_{x_1} & -\frac{r\kappa}{I}c_{x_2} & -\frac{r\kappa}{I}s_{x_2} & \frac{r\kappa}{I}c_{y_1} & \frac{r\kappa}{I}s_{y_1} & -\frac{r\kappa}{I}c_{y_2} & -\frac{r\kappa}{I}s_{y_2} \\ -l_{x1a} & -\frac{\kappa}{L}c_{x_1} & 0 & 0 & 0 & -\frac{r\kappa}{L}c_\theta c_{x_1} & -\frac{R}{L} & 0 & 0 & 0 & 0 & 0 & 0 & 0 \\ -l_{x1b} & -\frac{\kappa}{L}s_{x_1} & 0 & 0 & 0 & -\frac{r\kappa}{L}c_\theta s_{x_1} & 0 & -\frac{R}{L} & 0 & 0 & 0 & 0 & 0 & 0 \\ -l_{x2a} & -\frac{\kappa}{L}c_{x_2} & 0 & 0 & 0 & +\frac{r\kappa}{L}c_\theta c_{x_2} & 0 & 0 & -\frac{R}{L} & 0 & 0 & 0 & 0 & 0 \\ -l_{x2b} & -\frac{\kappa}{L}s_{x_2} & 0 & 0 & 0 & +\frac{r\kappa}{L}c_\theta s_{x_2} & 0 & 0 & 0 & -\frac{R}{L} & 0 & 0 & 0 & 0 \\ 0 & 0 & -l_{y1a} & -\frac{\kappa}{L}c_{y_1} & 0 & -\frac{r\kappa}{L}c_\theta c_{y_1} & 0 & 0 & 0 & 0 & -\frac{R}{L} & 0 & 0 & 0 \\ 0 & 0 & -l_{y1b} & -\frac{\kappa}{L}c_{y_2} & 0 & -\frac{r\kappa}{L}c_\theta s_{y_1} & 0 & 0 & 0 & 0 & 0 & -\frac{R}{L} & 0 & 0 \\ 0 & 0 & -l_{y2a} & -\frac{\kappa}{L}s_{y_1} & 0 & +\frac{r\kappa}{L}c_\theta c_{y_2} & 0 & 0 & 0 & 0 & 0 & 0 & -\frac{R}{L} & 0 \\ 0 & 0 & -l_{y2b} & -\frac{\kappa}{L}s_{y_2} & 0 & +\frac{r\kappa}{L}c_\theta s_{y_2} & 0 & 0 & 0 & 0 & 0 & 0 & 0 & -\frac{R}{L} \end{bmatrix}.$$

In the closed-loop system (31), A_m and A_e are Hurwitz with the positive control gains. B_{m_1}, B_{m_2}, and B_e are bouneded. Thus, e_m and e_e are ISS stable. In the previous section, it was proven that $\tilde{X}$ exponentially converge to zero. Thus, e_e converges to zero. Consequently, e_m converges to zero.

6. Simulation Results

We performed simulations to evaluate the performance of the proposed method. The simulations were performed using MATLAB/Simulink. The parameters of the planar motor, Normag XY1304, were used. The parameters, control gains, and observer gains used are listed in Table 1. The sampling frequency was set to be 1 MHz. To demonstrate the robustness of the proposed controller, the following disturbances of both forces and torque are included in the simulations.

- $F_{dx} = 14(1 + 0.5\cos(3t))\dot{x} + 2\sin(4\gamma x)$,
- $F_{dy} = 14(1 + 0.5\cos(3t))\dot{y} + 2\sin(4\gamma y)$,
- $\tau_d = 5(1 + 0.5\cos(2t))\dot{\theta}$.

In these simulations, the proposed method was compared to the conventional PID controller (32) as follows:

$$\begin{aligned} F_x &= k_{px}(x^d - x) + k_{ix}\int_0^t (x^d - x)d\tau + k_{dx}(\dot{x}^d - \dot{x}) \\ F_y &= k_{px}(y^d - y) + k_{iy}\int_0^t (y^d - y)d\tau + k_{dy}(\dot{y}^d - \dot{y}) \\ \tau &= k_{p\theta}(\theta^d - \theta) + k_{i\theta}\int_0^t (\theta^d - \theta)d\tau + k_{dy}(\dot{\theta}^d - \dot{\theta}), \end{aligned} \tag{32}$$

where $k_{px} = k_{py} = 50,000$, $k_{dx} = k_{dy} = 50$, $k_{ix} = k_{iy} = 500$, $k_{p\theta} = 1000$, $k_{d\theta} = 5$, and $k_{i\theta} = 2000$. Two cases were tested to evaluate the effect of the proposed method, which are as follows:

- Case 1: The conventional PID controller (32) and the nonlinear controller (24).
- Case 2: The proposed controller (16) and (24) with the constraints ($b_x, b_y, b_\theta = 1 \times 10^{-5}$).

For two cases, the commutation scheme (17) and the nonlinear observer (26) were used.

Table 1. Plant parameters, control gains, and observer gains.

Plant Parameters and Gains		
Plant parameters	M	1.35 kg
	I	4×10^{-3} kg/m^2
	r	0.0485 m
	γ	$2 * \pi / p$
	p	1.0168 mm
	κ	17
	L	7×10^{-4} H
	R	2 Ω
Control gains	k_x, k_y	1×10^{10}
	k_θ	3×10^{17}
	k_{x_v}, k_{y_v}	1×10^{4}
	k_{θ_v}	6×10^{3}
	ρ	1×10^{5}
Observer gains	l_x, l_y	1000
	l_θ	20,000
	l_{xv}, l_{yv}	5.18×10^{-4}
	$l_{\theta v}$	0.175
	l_{x1a}, l_{x1b}	0
	l_{x2a}, l_{x2b}	0
	l_{y1a}, l_{y1b}	0
	l_{y2a}, l_{y2b}	0

The desired positions for X and Y directions as shown in Figure 2 are used. The desired yaw was set to be zero.

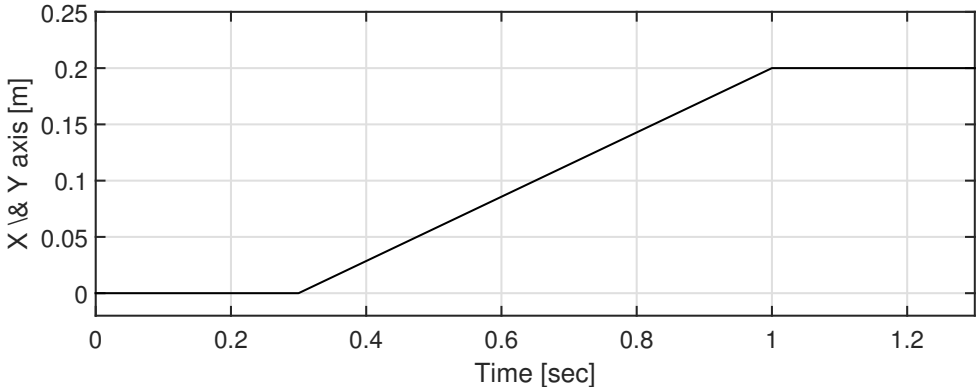

Figure 2. Desired positions for X and Y directions.

The estimation performances of x, y, θ, and i for Case 2 are shown in Figures 3 and 4. It is observed that the estimated states tracked well the actual states by using the proposed nonlinear observer.

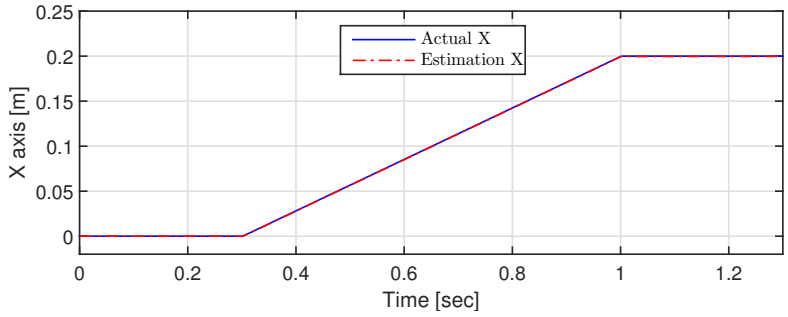

(**a**) Estimation of x

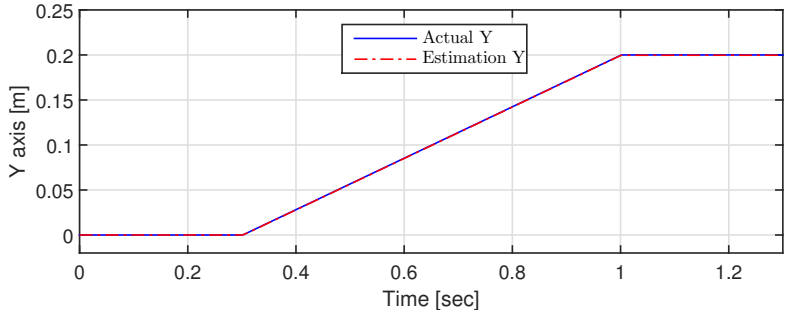

(**b**) Estimation of y

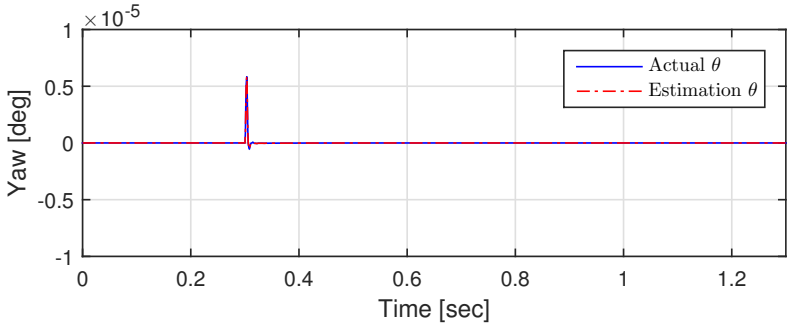

(**c**) Estimation of θ

Figure 3. Estimation performances of x, y, θ for Case 2.

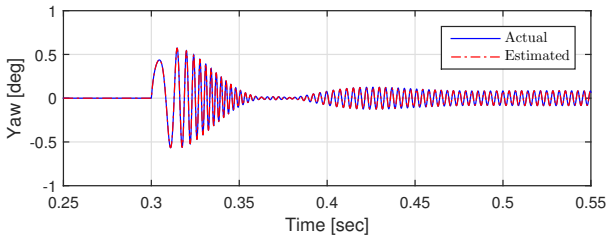

(**a**) Estimation of i_{x1a}

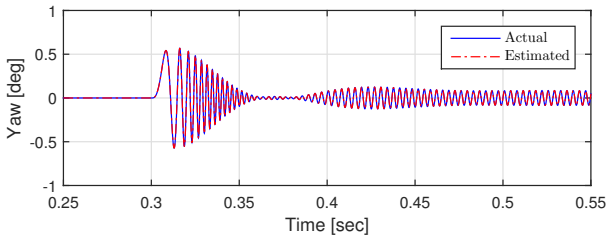

(**b**) Estimation of i_{x1b}

Figure 4. Estimation performances of i_{x1a} and i_{x1b} for Case 2.

Figures 5–7 show the simulation results for cases 1 and 2. Large acceleration and deceleration appear in the desired positions for the X and Y directions. Thus, large overshoots of the positions and yaw appear in case 1. The offset error in the positions exist during periods of constant velocity. Moreover, in case 2, the tolerances 1×10^{-5} for the position tracking errors and yaw are guaranteed by the proposed method during both transient and constant periods. Furthermore, the offset error in the positions disappeared during the constant velocity periods.

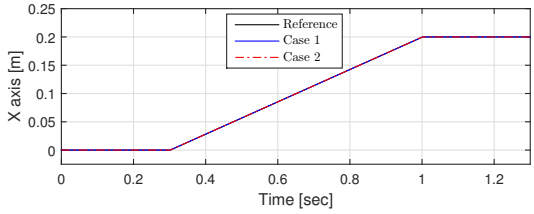

(**a**) Tracking performance

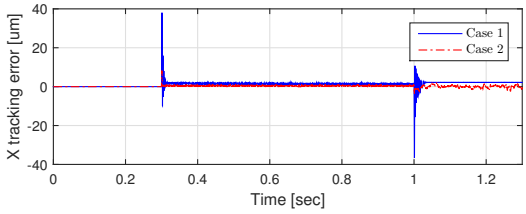

(**b**) Tracking error

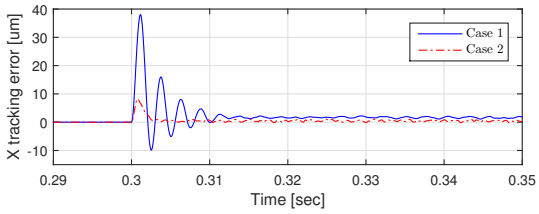

(**c**) Zoom-out of tracking error

Figure 5. Tracking performance for X direction for cases 1 and 2.

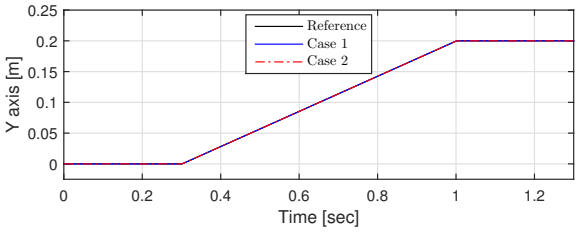

(**a**) Tracking performance

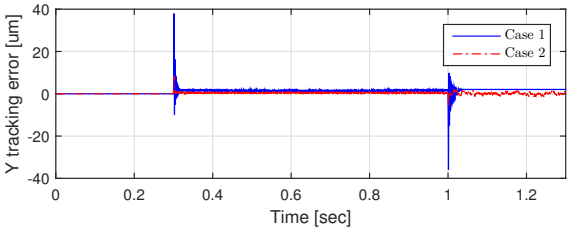

(**b**) Tracking error

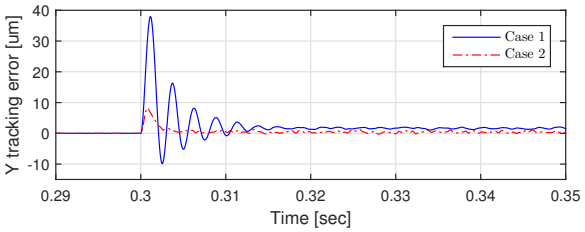

(**c**) Zoom-out of tracking error

Figure 6. Tracking performance for Y direction for cases 1 and 2.

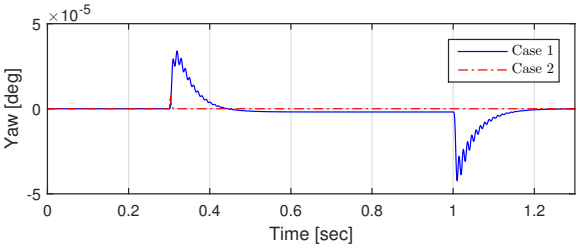

(**a**) Yaw

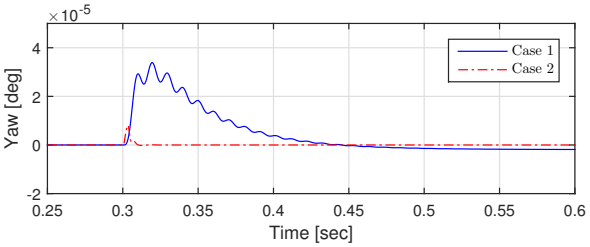

(**b**) Zoom-out of yaw

Figure 7. Yaw regulation performance for cases 1 and 3.

7. Conclusions

In this paper, we proposed nonlinear position control using only position feedback to guarantee the tolerances for position tracking errors and yaw in air-bearing planar motors. The proposed method consisted of the nonlinear position controller and nonlinear observer. The nonlinear position controller was designed by a backstepping procedure using BLF to satisfy the constraints of position errors and yaw. The nonlinear observer was developed to estimate full state using only position feedback. In the simulations, we observed that the tolerances for the position tracking errors and yaw were guaranteed by the proposed method during both transient and constant periods. In the future work, we will design the controller to guarantee the constraints of both the control inputs and the outputs.

Author Contributions: Conceptualization, W.K. and D.S; validation, D.S.; writing–original draft preparation, W.K.; writing—review and editing, Y.L. All authors have read and agreed to the published version of the manuscript.

Funding: This research was supported by Energy Cloud R&D Program through the National Research Foundation of Korea (NRF) funded by the Ministry of Science, ICT (2019M3F2A1073313) and also supported by asic Science Research Program through the National Research Foundation of Korea (NRF) funded by the Ministry of Education (2020R1I1A3073378).

Conflicts of Interest: The authors declare that they have no conflicts of interest.

References

1. Ro, S.-K.; Park, J.-K. A compact ultra-precision air bearing stage with 3-DOF planar motions using electromagnetic motors. *Int. J. Prec. Eng. Manuf.* **2011**, *12*, 115–119. [CrossRef]
2. Melkote, H.; Khorrami, F.; Ish-Shalom, J. Closed-loop control of a three degree-of-freedom ultra accurate linear stepper motor. In Proceedings of the 1997 IEEE International Conference on Control Applications, Hartford, CT, USA, 5–7 October 1997; pp. 639–644.
3. Quaid, A.E.; Hollis, R.L. 3-DOF closed-loop control for planar linear motors. In Proceedings of the 1998 IEEE International Conference on Robotics and Automation, Leuven, Belgium, 20–20 May 1998; pp. 2488–2493.
4. Melkote, H. Khorrami, F. Closed-loop control of a base XY stage with rotational degree-of-freedom for a high-speed ultra-accurate manufacturing system. In Proceedings of the 1999 IEEE International Conference on Robotics and Automation, Detroit, MI, USA, 10–15 May 1999; pp. 1812–1817.
5. Krishnamurthy, P.; Khorrami, F.; Ng, T.L.; Cherepinsky, I. Control design and implementation for Sawyer motors used in manufacturing systems. *IEEE Trans. Control Syst. Technol.* **2011**, *19*, 1467–1478. [CrossRef]
6. Nguyen, V.H.; Kim, W.-J. Design and control of a compact lightweight planar positioner moving over a concentrated-field magnet matrix. *IEEE/ASME Trans. Mechatron.* **2013**, *18*, 1090–1099. [CrossRef]
7. Hu, C.; Wang, Z.; Zhu, Y.; Zhang, M.; Liu, H. Performance-oriented precision LARC tracking motion control of a magnetically levitated planar motor with comparative experiments. *IEEE Trans. Ind. Electron.* **2016**, *63*, 5763–5773. [CrossRef]
8. Huang, S.; Chen, L.; Cao, G.; Wu, C.; Xu, J.; He, Z. Predictive position control of planar motors using trajectory gradient soft constraint with attenuation coefficients in the weighting matrix. *IEEE Trans. Ind. Electron.* **2020**. [CrossRef]
9. Sapuppo, F.; Llobera, A.; Schembri, F.; Intaglietta, M.; Cadarso, V.J.; Bucolo, M. A polymeric micro-optical interface for flow monitoring in biomicrofluidics. *J. Biomicrofluid.* **2010**, *4*, 024108 [CrossRef] [PubMed]
10. Liu, K.; Li, K.; Zhang, C. Constrained generalized predictive control of battery charging process based on a coupled thermoelectric model. *J. Power Source* **2017**, *347*, 145–158 [CrossRef]
11. Liu, K.; Li, K.; Ma, H.; Zhang, J.; Peng, Q. Multi-objective optimization of charging patterns for lithium-ion battery management. *Energy Convers. Manag.* **2018**, *159*, 151–162. [CrossRef]
12. Liu, K.; Zou, C.; Li, K.; Wik, T. Charging pattern optimization for lithium-ion batteries with an electrothermal-aging model. *IEEE Trans. Ind. Inform.* **2018**, *14*, 5463–5474. [CrossRef]
13. Liu, K.; Hu, X.; Yang, Z.; Xie, Y.; Feng, S. Lithium-ion battery charging management considering economic costs of electrical energy loss and battery degradation. *Energy Convers. Manag.* **2019**, *195*, 167–179. [CrossRef]
14. Ouyang, Q.; Wang, Z.; Liu, K.; Xu, G.; Li, Y. Optimal charging control for lithium-ion battery packs. *IEEE Trans. Ind. Inform.* **2020**, *16*, 3430–3438. [CrossRef]

15. Kim, W.; Shin, D.; Chung, C.C. The Lyapunov-based controller with a passive nonlinear observer to improve position tracking performance of microstepping in permanent magnet stepper motors. *Automatica* **2012**, *48*, 3064–3074. [CrossRef]
16. Krishnamurthy, P.; Khorrami, F. Robust adaptive control of Sawyer motors without current measurements. *IEEE Trans. Mechatron.* **2004**, *9*, 689–696. [CrossRef]
17. Bodson, M.; Chiasson, J.; Novotnak, R.; Rekowski, R. High performance nonlinear feedback control of a permanent magnet stepper motor. *IEEE Trans. Control Syst. Technol.* **1993**, *1*, 5–14. [CrossRef]